Journal of Sound and Vibration (1999) **226**(2), 285–304
Article No. jsvi.1999.2294, available online at http://www.idealibrary.com on IDEAL®

POWER OUTPUT OF NOISE SOURCES OPERATING NEAR ELASTIC SCATTERERS OF FINITE DIMENSIONS

T. M. TOMILINA,† YU. I. BOBROVNITSKII, V. B. YASHKIN AND A. A. KOCHKIN

Laboratory of Structural Acoustics, Mechanical Engineering Research Institute, (IMASH), M. Kharitonyevsky 4, 101830 *Moscow, Russia*

(*Received* 10 *July* 1998, *and in final form* 29 *March* 1999)

The problem of variation of the sound power output of noise sources due to reflecting boundaries and elastic scatterers is considered experimentally and numerically. In the laboratory experiment with a source of loudspeakers operating near a resonant scatterer, the increase in the radiated power obtained is about one hundred. An important role of the source near field in the power enhancement is shown. In computer simulation, a two-dimensional radiation problem for a circle vibrating near a finite elastic beam is studied. Most attention is paid to revealing physical mechanisms of the power output variations. It is shown that, for the source and elastic scatterer of finite dimensions, the radiated power can reach orders of magnitude of the free-field value. Especially, high-power amplification can be obtained at low frequencies for the sources that are poor radiators in free space, i.e., behave as multipoles of high order: presence of a scatterer or reflector makes such a source to be of monopole or dipole type. The results presented can be useful in better understanding sound generation mechanisms in complicated industrial noise sources.

1. INTRODUCTION

The sound power radiated from a noise source is an important parameter characterizing ability of physical objects to generate sound. For measuring the power, there exist appropriate methods and facilities [1]. The power output is used as an input parameter in some noise level prediction techniques based on the energy balance equations, in the Statistical Energy Analysis (SEA) in particular [2], where it is assumed to vary slightly in different acoustic environments.

At the same time, there are practical situations in which the power output of sound sources is amplified or reduced markedly due to the presence of elastic bodies and boundaries. Studying such situations and revealing the physical

† This work was carried out during the autor's guest research period at the Department of Applied Acoustics, Chalmers University of Technology, 41296 Gothenburg, Sweden. The experiment was done at the Laboratory of Structural Acoustics, IMASH, 101830 Moscow, Russia.

0022-460X/99/370285 + 20 $30.00/0

mechanisms underlying the power variation is the main objective of the present paper. Among the infinite diversity of acoustical sources and environments, the present study is confined to the sources modelled by geometric objects with the vibrating surfaces which radiate sound into the fluid-filled space bounded by reflecting planes and containing elastic bodies (scatterers). It is supposed that the source and scatterer interact only via the fluid, and the effect of variation of the source power output is caused by this fluid coupling.

In the literature on the subject, a review of which will be published elsewhere, the effect of amplification or reduction of the sound power output has been studied for point sources (see, e.g., references [3–5] or, partly, line sources [6] which are acoustically transparent and cannot scatter sound waves. For such sources, the physical mechanisms backing the effect are (1) *interference* of direct and reflected waves and (2) *reradiation* of sound by acoustically more efficient resonant scatterers, e.g., by air bubbles in water. However, for more complicated sound sources there are other physical mechanisms giving power enhancement. In particular, for sources of finite dimensions having impervious surfaces which can scatter sound waves, multiple scattering of the waves by such a source and foreign body or boundary produces resonance and antiresonance of the fluid volume between the source and reflecting surface and, consequently, leads to amplification or reduction of the source power output. This physical mechanism, called *cavity resonance*, was first studied in reference [7]: for a circular disc pulsating or oscillating near a rigid wall, the radiation power amplification exceeds 10 at the cavity resonance frequencies while pure interference can not provide more than 2.

Finite dimensions of the source and multiple scattering give rise to one more physical mechanism of the power output amplification—*source order lowering*. It works at low frequencies with the sources that are very inefficient in free space (behave as multipoles of high orders). Bringing a foreign object into the vicinity of such a source makes it much more efficient (lowers its order). The power amplification can reach orders of magnitude. This physical mechanism is one of the main findings of the present work.

The paper consists of two parts. In the first part (section 2), a laboratory experiment which confirms the theoretical predictions of reference [7] concerning resonant scattering is described. It has been shown in the experiment that the effect of the sound power enhancement is of practical importance: the measured radiation power amplification of the real sources reaches two orders of magnitude.

In the second part of this paper (section 3), a two-dimensional radiation problem for a source and scatterer of finite dimensions (a circle near flexurally vibrating beam) are considered theoretically and numerically. This acoustical configuration is close to some practical noise sources, e.g., vibrating machine members radiating sound near elastic structures. Several physical mechanisms work simultaneously in this configuration. Where possible, they are separated and their contributions are estimated quantitatively. At the end of the paper the main results are summarized and some possible applications are pointed out.

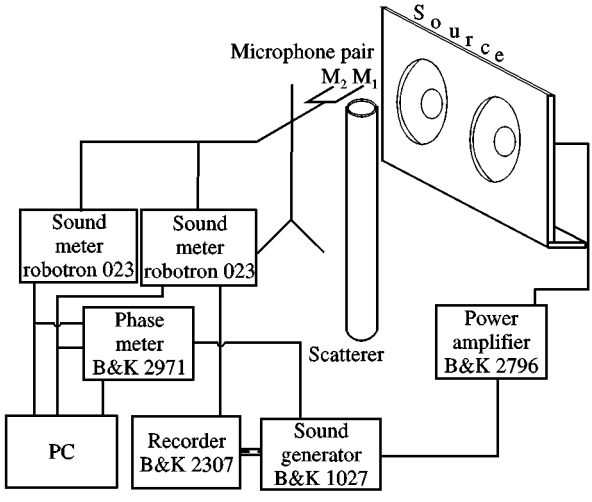

Figure 1. Experimental set-up.

2. EXPERIMENTAL STUDY OF RESONANT SCATTERING

The aim of the experiment is two-fold: to verify that a considerable increase in the power output can take place for real sound sources and to show the important role of the source reactive near field in this physical effect.

2.1. SOUND SOURCE

A special sound source was designed for the purpose of this experiment. It consists of two identical loudspeakers of diameter 28 cm mounted in a wooden finite baffle with dimensions in $75 \times 45 \times 1{\cdot}5$ cm (see Figure 1). It has two regimes of work: in the first regime, the cones of the loudspeakers move in phase; in the second regime, they move in counter-phase. At low frequencies, the field of the source in the in-phase regime is close to the field of a dipole source and in the counter-phase regime it resembles the field of a lateral quadrupole. The source could thus generate two types of acoustic fields with different reactive components. This allows one to study the influence of the nearfield characteristics on the amount of the sound power output.

2.2. EXPERIMENTAL SET-UP

The schematic of the experiment conducted is presented in Figure 1. The sound source was excited by harmonic signals from a sound generator. A steel pipe (height 91 cm, inner diameter 11 cm, wall thickness 0·4 cm) was placed near the source. One end of the pipe was closed, the other end could be closed (in this case, the pipe represented a rigid cylindrical scatterer of low efficiency) or it could be open in which case the pipe served as an effective resonant scatterer with the main eigenfrequency about 91·7 Hz. The pressure field was picked up by 1/4-in microphones RFT MK201. The intensity was measured by two microphones

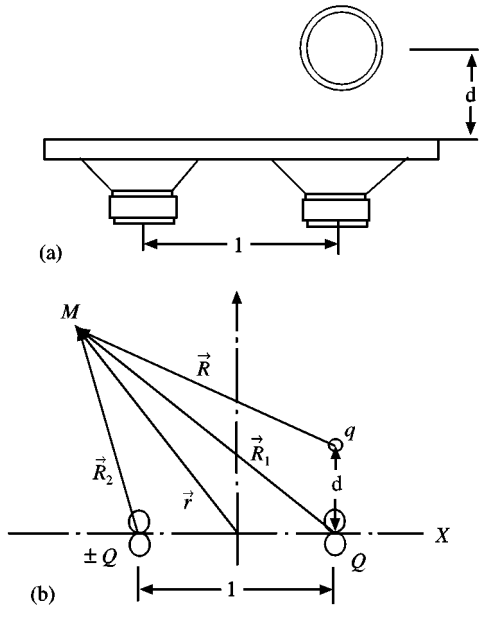

Figure 2. Acoustic sources (a) and their models (b).

spaced at 12 cm. The total power output of the source was obtained by measuring the intensity at 162 points on a closed cylindrical surface (diameter 2 m, height 1·6 m) enveloping the source and the scatterer. The experiment has been carried out in a hall with dimensions $12 \times 6 \times 6$ m. The ceiling and walls were covered by sound-absorbing material with the surface absorption coefficient of about 20% at the frequency 100 Hz. The loudspeakers and the open end of the pipe were situated in a horizontal plane at the level 1 m above the floor.

2.3. ACOUSTIC FIELD AND SOURCE MODELS

In the measurement frequency range 80–120 Hz, the sound wavelength in air is much greater than the dimensions of the source and pipe diameter. Therefore, in theoretical consideration, each loudspeaker was modelled by a dipole source and the open end of the pipe was modelled by a monopole source (see Figure 2). Thus, the acoustic field in the experiment was represented by the sum of the point sources fields,

$$p(\mathbf{r}) = p_{d_1}(\mathbf{r}) + p_{d_2}(\mathbf{r}) + p_m(\mathbf{r}), \tag{1}$$

where

$$P_m(\mathbf{r}) = q \cdot g_m(\mathbf{r}|\mathbf{r}_m) \tag{2}$$

is the field of a monopole source with the volumetric velocity q and the Green function

$$g_m(\mathbf{r}|\mathbf{r}_m) = \frac{1}{4\pi}\rho c k^2 [\mathrm{h}_0(kR) + \mathrm{h}_0(kR')]$$

and

$$p_{d_j}(\mathbf{r}) = Q g_{d_j}(\mathbf{r}|\mathbf{r}_{d_j}) \tag{3}$$

is the field of a dipole source oriented along the unity vector $\mathbf{n}$ with the dipole moment Q and the field function

$$g_{d_j}(\mathbf{r}|\mathbf{r}_{d_j}) = \frac{1}{4\pi}\rho c k^3[(\mathbf{n}\mathbf{v}_j)\mathrm{h}_1(kR_{d_j}) + (\mathbf{n}'\mathbf{v}'_j)\mathrm{h}_1(kR'_{d_j})].$$

Here $\mathbf{r}$, $\mathbf{r}_m$ and $\mathbf{r}_{d_j}$ are vectors to an observation point and to the monopole and dipole sources locations, $\mathbf{R} = \mathbf{r} - \mathbf{r}_m$, $\mathbf{R}_{d_j} = \mathbf{r} - \mathbf{r}_{d_j}$, $R = |\mathbf{R}|$, $\mathbf{v}_j = \mathbf{R}_d/R_{d_j}$, $j = 1, 2$ (see Figure 2); ρ, c and k are the density, speed of sound and wave number for air; h_0 and h_1 are the spherical Bessel functions; the factor $\exp(-\mathrm{i}\omega t)$ is omitted throughout the paper. The field functions of the monopole and dipole sources in equations (2) and (3) take into account the reflection from the floor using the fields of the corresponding image monopole and dipole sources located at the points $\mathbf{r}'_m$ and $\mathbf{r}'_{d_j}$ symmetrically to the points $\mathbf{r}_m$ and $\mathbf{r}_{d_j}$ with respect to the floor plane, $\mathbf{R}' = \mathbf{r} - \mathbf{r}'_m$, $\mathbf{R}'_{d_j} = \mathbf{r} - \mathbf{r}'_{d_j}$. Reflections from the ceiling and walls were neglected.

The unknown parameters of the described model q and Q were defined as follows. The volumetric velocity q of the monopole source in equation (2) is equal to $q = vS$, where S is the cross-sectional area of the pipe and v is the complex amplitude of the air particle mean velocity at the opening of the pipe. The latter was computed as a result of the forced vibrations of the air column inside the pipe connected with the exterior air under the action of the incident field which in this case is equal to $p_{d_1} + p_{d_2}$ in equation (1).

The most important and uncertain parameter here is the loss factor of the pipe vibration caused by radiation of sound into the open air and by the viscous damping in the air flow about the pipe edge and walls. As it turned out, the radiation losses alone (a theoretical estimate is equal to $\eta_{\mathrm{rad}} = 0{\cdot}003$) are not sufficient for describing the experimental data. Therefore, the actual value of the loss factor $\eta = 0{\cdot}013$ was identified via fitting the theoretical amplitude versus frequency curve to the corresponding experimental dependence by minimizing the discrepancy between them. Another model parameter, the dipole moment Q, due to the difficulties of its theoretical estimation, was also identified from the experimental data in a similar manner.

The accuracy of the field model (1) was proved to depend on the distance from the source. At the distance $r = 0{\cdot}5$ m, the relative error of description of the measured pressure field was less than 15%. At the distance $r = 1{\cdot}5$ m from the source this error equalled 25%. The increase in the error with the distance can be attributed to reflection from the walls which was not taken into account in the model.

2.4. EXPERIMENTAL RESULTS

Figures 3 and 4 show the pressure amplitudes for the two sources with and without the resonant scatterer. These data correspond to measurements at the frequency 91·7 Hz of the open-pipe first resonance. With the pipe closed, the angle

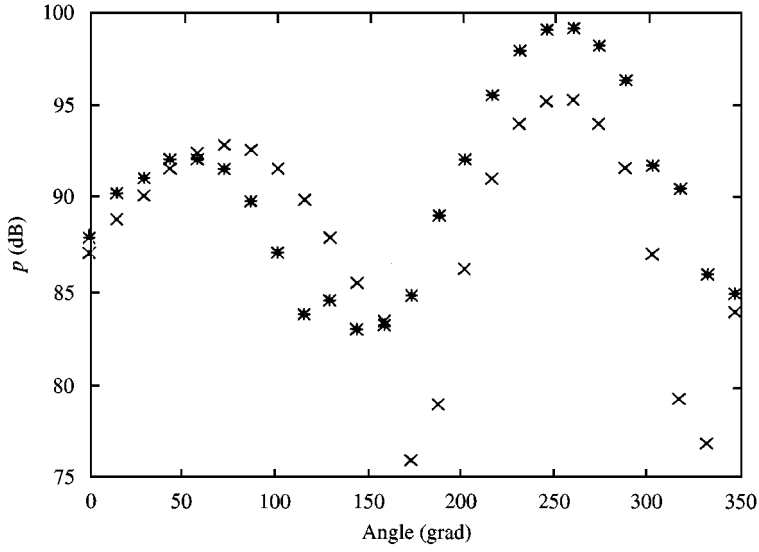

Figure 3. Experimental angle distribution of the sound pressure amplitude along a horizontal circle of diameter 2 m for the in-phase regime of the source: +, without resonant scatterer (pipe end closed); *, with resonant scatterer (pipe end open).

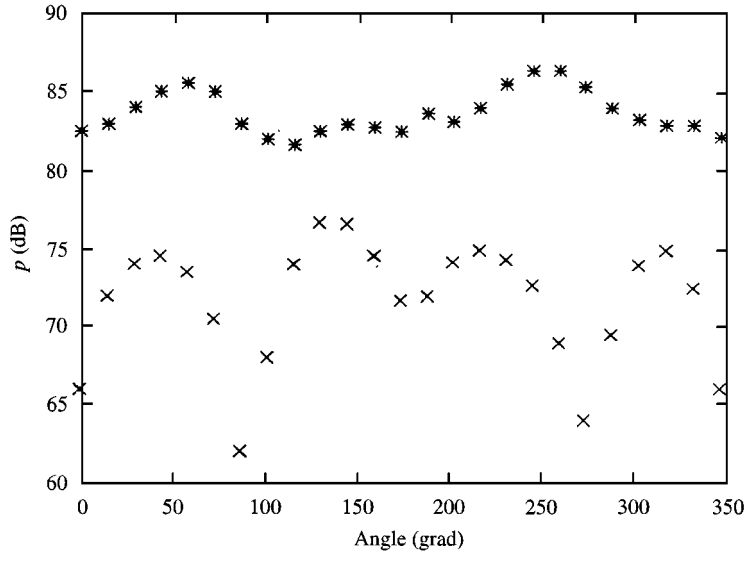

Figure 4. The same as in Figure 3 for the counter-phase regime of the sound source.

dependencies in Figures 3 and 4 (crests) are similar to the directivity patterns of a dipole source (two lobes) and lateral quadrupole source (four lobes). Placing the resonant scatterer (opening the pipe) increases the pressure field (stars), especially for the counter-phase regime, and makes the field almost omnidirectional since the scattering component of the field is of the monopole type. As seen from Figures 3 and 4, the scattered pressure field, that is to say the difference between the pressure

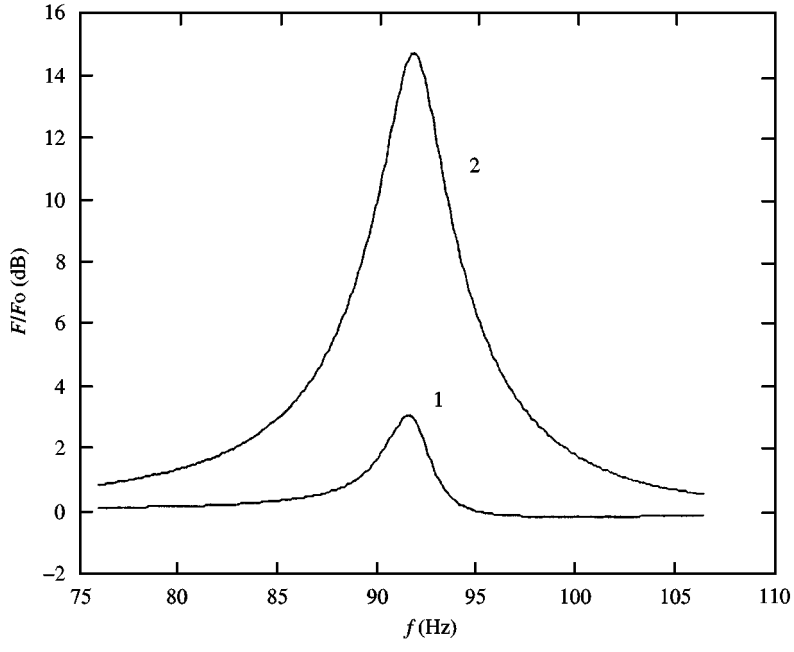

Figure 5. Power ratio (4) of the source versus frequency for the in-phase regime (1) and counter-phase regime (2).

fields with and without the scatterer, is not uniform in space and cannot be a reliable measure of the field amplification. The same is valid for the intensity distribution in space. So, the total power output of the source was adopted as the measure of the field amplification effect which is considered further in the paper.

Figure 5 presents a frequency dependency of the power ratio PR in dB defined as

$$PR = 10\log(F/F_0), \tag{4}$$

where F_0 is the radiation power of the source without the scatterer and F is that with the scatterer. The curves in Figure 5 are computed for the model in Figure 2(b) and correspond to the distance $d = 22$ cm between the source and scatterer. The peaks on the curves are at the frequency of the pipe resonance.

In Figure 6 the power ratio (4), corresponding to the resonance frequency, is shown as a function of distance d. Two main features are seen in this figure. First, the experiment clearly shows that there exists an increase in the power output of the real source (loudspeakers, in our case). For short distances between the source and the scatterer, the power amplification is almost *two orders*. This is large enough to be of practical importance.

Another feature of Figure 6 is the striking difference between the results for the two regimes of work of the sound source. This can be explained as follows. The scattered sound power is proportional to the squared amplitude of the incident pressure field. A quadrupole sound source has a near field much stronger than that of dipole source. Therefore, the sound source used in the experiment working in the

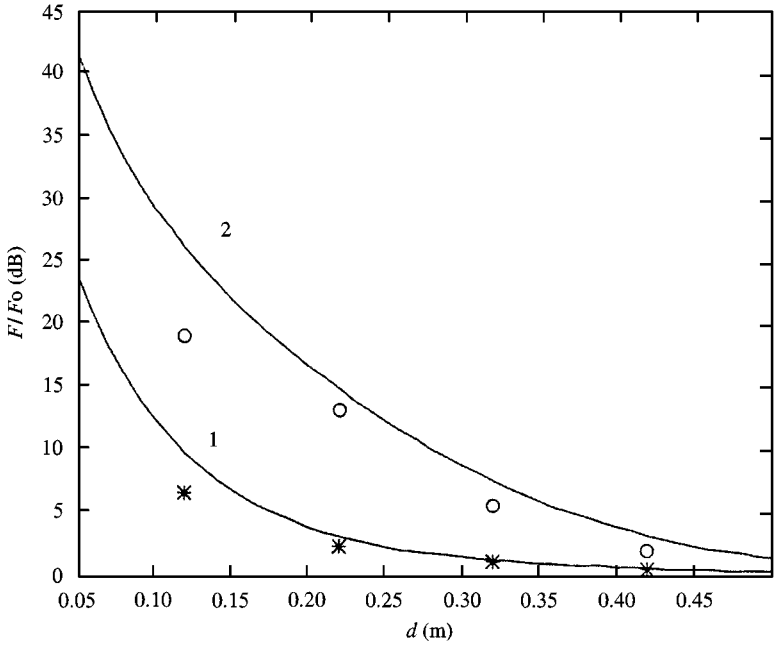

Figure 6. Power ratio (4) versus distance d between the source and the scatterer at the resonance frequency of the scatterer: solid lines correspond to prediction. * and ○ are experimental results for the in-phase and counter-phase regimes respectively.

counter-phase regime has much greater pressure amplitude in the near field than in the in-phase regime. Consequently, the scattered field and amplification is much greater in the counter-phase regime.

2.5. PHYSICS OF POWER AMPLIFICATION

When the power output of a source increases it means that an additional amount of the acoustic energy is radiated into the space. The answer to the question "Where is the additional energy taken from" is evident from the energy conservation law: it is taken from the sound source since the scatterer is assumed to be "passive" and does not contain energy sources or sinks. The physics of the power output increase is as follows. When a scatterer is placed near the source, the scattered field produces additional pressure at the source surface and thus changes the radiation impedance, including its real part, the radiation resistance.

For sources of the Neumann type which are used in the computational model in Figure 2(b), the kinematic source parameters q and Q remain constant, so that an increase in the radiation resistance leads to a proportional increase in the sound power output. The loudspeakers in the experiment were not exactly sources of the Neumann type. The velocity amplitude directly measured at the loudspeaker cones decreased when the scatterer was present. The decrease reached 15%. Nevertheless, significant increase in the radiated power, though not as high as predicted by the Neumann's model, took place in the experiment.

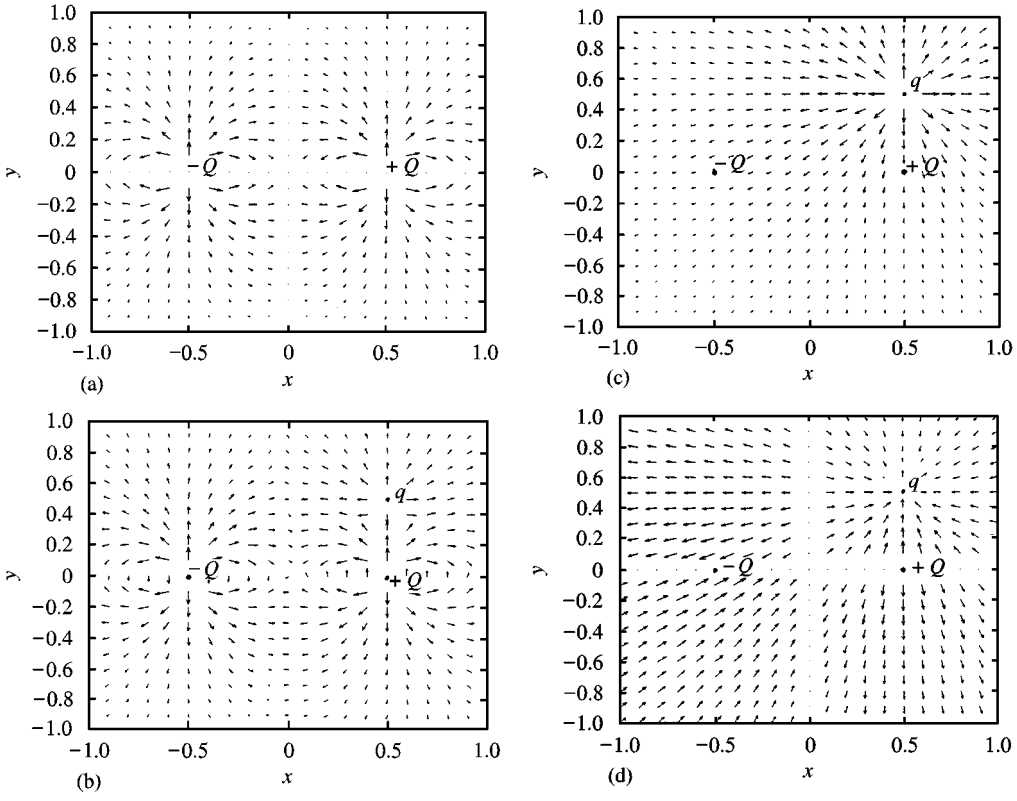

Figure 7. Intensity maps of the field of the point acoustic sources shown in Figure 2(b): (a) incident field (field of two dipoles): (b) total field (field of two dipoles and monopole); (c) scattered field (field of the monopole); (d) cross-intensity.

The physics of the sound power increase can also be visualized with the help of the vector fields of the intensity. Figure 7 shows various components of the full intensity map computed for the plane in which two model dipoles and monopole lie —see Figure 2(b). They correspond to the resonance frequency of the pipe and to the source working in the counter-phase regime. Figure 7(a) shows the intensity of the incident component of the field (source without scatterer), Figure 7(b) the resulting field (source with scatterer), Figure 7(c) the scattered component of the field, and Figure 7(d) the field of the cross-intensity, i.e., the active power of the pressure of the incident field on the particle velocity of the scattered field. It is seen that the additional power is delivered to the scatterer via the cross- intensity flow, Figure 7(d), and then it is radiated with the scattered field, Figure 7(c).

3. RADIATION OF A CIRCLE NEAR A FINITE ELASTIC BEAM

The following two-dimensional radiation problem is considered numerically in this section: a vibrating circle radiates sound near a thin finite elastic beam. The

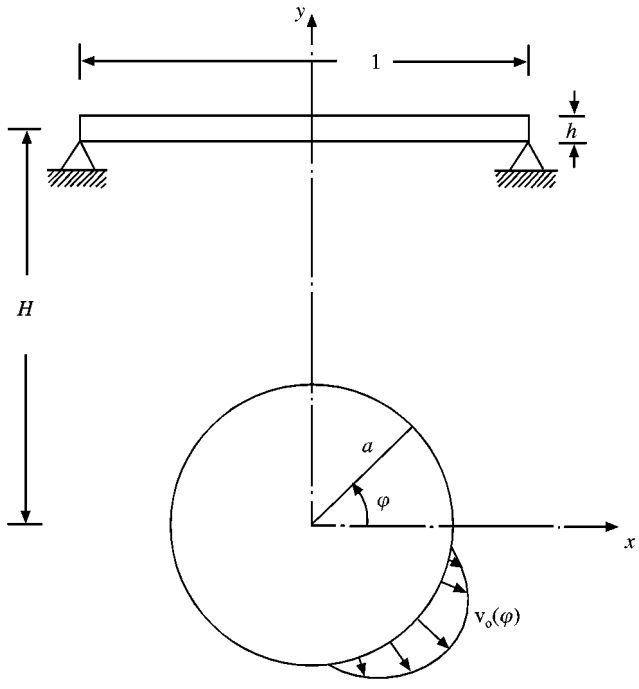

Figure 8. A circle vibrating with prescribed velocity near a simply supported beam.

purpose of the consideration is to study the properties (mostly, amplification) of the sound power output in the situation when both the source and scatterer are of finite dimensions (so that multiple scattering is possible) and when the scatterer is elastic, i.e., has a set of eigenfrequencies and normal modes (so that the resonant scattering is possible). This two-dimensional problem is identical to the three-dimensional problem for an infinite circular cylinder and thin strip if the cylinder vibration and all the acoustic variables are uniform along the axial co-ordinate.

3.1. FORMULATION OF THE PROBLEM

The circle has radius a, the beam is of length l and thickness h (see Figure 8). Both Cartesian (x, y) and polar (r, φ) co-ordinates with the origin at the center of the circle are used. The circle is a sound source of the Neumann type: the radial velocity is prescribed on its contour,

$$v_r(a, \varphi) = v_0(\varphi), \tag{5}$$

with $v_0(\varphi)$ being a given distribution function.

The beam performs forced flexural vibrations under the action of the pressure field produced by the circular source and, thus, reradiates or scatters sound into the boundless medium. The thickness h is assumed small compared with the flexural

wavelength, and the governing equation for the beam flexural vibrations is the classical equation of Bernoulli–Euler [8],

$$Lw(x) = B\partial^4 w/\partial x^4 - \rho_b h\omega^2 w = \Delta p(x), \tag{6}$$

where $w(x)$ is the lateral displacement, $B = EI$ is the bending rigidity, $I = h^3/12$ is the second moment of the beam cross-section, ρ_b is the density of the beam material, the Young's modulus is assumed to be complex $E = E_0(1 - i\eta)$ with the material loss factor η, and $\Delta p(x)$ is the pressure difference on the lower and upper sides of the beam:

$$\Delta p(x) = p(x, H - h/2) - p(x, H + h/2).$$

A solution of equation (6) must satisfy boundary conditions at the beam ends which are supposed to be simply supported:

$$w(\pm l/2) = w''(\pm l/2) = 0. \tag{7}$$

The flexural operator (6), (7) can be rewritten in the equivalent integral form

$$v(x) = \int_{-l/2}^{l/2} G(x/\xi)\Delta p(\xi)\,\mathrm{d}\xi, \tag{8}$$

where $v = \dot{w}$ is the lateral beam velocity and $G(x/\xi)$ is the Green function of the beam in vacuum satisfying the equation $Lv = -i\omega\delta(x - \xi)$ and the boundary conditions (7), $\delta(\ )$ being the Dirac delta function.

Mathematically, the problem is formulated as follows: find a solution of the Helmholtz equation $\Delta p + k^2 p = 0$ (k is the acoustic wavenumber) which satisfies the boundary condition (5) on the circle contour, equation (8) on the upper and lower sides of the beam, and the Sommerfeld radiation condition at the infinity. The integral flexural operator (8) is used here instead of the differential operator (6), (7) for the sake of computational convenience—see reference [9].

The Green function of the beam in vacuum in equation (8) can be derived in the usual way [8] in the form of an expansion in normal modes. The beam normal modes ($n = 1, 2 \ldots$)

$$v_n(x) = \sqrt{\frac{1}{l}}\sin\frac{\pi n(x + l/2)}{l} \tag{9}$$

are orthogonal and normalized. Upon introducing the real-valued flexural wavenumber k_0 ($k_0^4 = \rho_b h\omega^2/E_0 I$), the Green function can be written, after some manipulations, in the form

$$G(x/\xi) = G_0 \sum_{n=1}^{\infty} \frac{v_n(x)v_n(\xi)}{(k_0 l) - (n\pi)^4(1 - i\eta)} \tag{10}$$

with $G_0 = i\omega l^4/E_0 I$. The series in equation (10) converges very rapidly as n^{-4}, so that if the frequency is in the vicinity of the n_0th resonance ($k_0 l = \pi n_0$), it is sufficient to compute the sum of $3n_0$ first terms in equation (10) to obtain an approximate Green function which differs from the exact one ($n \to \infty$) by no more than 1%.

3.2. METHOD OF THE SOLUTION

The problem is solved by the modification of the Equivalent Sources Method (ESM) applicable to radiation problems for forced vibrating elastic structures [10]. According to this method, the circle and beam are removed from the medium and replaced by a set of equivalent point sources: the circle is replaced by $2N_1$ multipole point sources located at the center of the circle, the beam is replaced by N_2 dipole point sources equidistantly placed at the central line of the beam and oriented along the y-axis. The pressure field of the set of the equivalent multipole sources with amplitudes a_n and b_n is equal to

$$p_1(\mathbf{r}) = \sum_{n=0}^{N_1-1} (a_n \cos n\varphi + b_n \sin n\varphi) \mathrm{H}_n(kr), \tag{11}$$

the pressure field of the equivalent dipole sources with the amplitudes c_m is

$$p_2(\mathbf{r}) = \sum_{m=1}^{N_2} c_m \mathrm{H}_1(kR_m) \sin \varphi. \tag{12}$$

Here $\mathrm{H}_n(\ )$ is the Hankel function of the first kind of order n and R_m is the vector from mth dipole source to the observation point. The total pressure field of the problem is, thus, modelled by the sum of fields (11) and (12),

$$p_1(\mathbf{r}) = p_1(\mathbf{r}) + p_2(\mathbf{r}), \tag{13}$$

which contains $N = 2N_1 + N_2$ unknown model parameters–amplitudes of the equivalent sources, a_n, b_n and c_m. Using the pressure field representation (11)–(13), one can compute the amplitudes of the radial particle velocity at M_1 points of the circular contour, and y-component of velocity at M_2 points of the beam sides, and, after substituting them into the boundary conditions (5) and (8), obtain a set of $M = M_1 + M_2$ linear algebraic equations with $N < M$ unknowns. The solution of this set (the singular-value decomposition method was used) gives the amplitudes of the equivalent sources in the model (11)–(13). After that, any characteristics of the acoustic and vibration fields can be computed directly from equation (13).

It should be noted that the representation (11) of a two-dimensional sound field by a superposition of the outgoing cylindrical waves, known for $N_1 \to \infty$ as the Rayleigh series, is rather common and often used in acoustics and electromagnetic theory [11, 12]. The Rayleigh series is mathematically correct on the exterior of a circle enveloping the source. The truncated series (11) gives an approximation, the error depending on the number $2N_1$ of the multipole sources used.

The representation (12) of an acoustic field of a transversely vibrating beam by a set of point dipole sources is based on the well-known fact that any oscillating rigid body of small wave dimensions, as well as each element of the thin beam under study, is acoustically equivalent to a dipole point source. An extended thin beam can be correctly modelled by dipole sources distributed continuously along the beam central line. Its discretization, i.e., replacing it by a finite number of point dipole sources, as is done in representation (12), leads to an error which depends on the number N_2 of these point sources [9].

Practically, the numbers N_1 and N_2 of the equivalent sources were determined in the work by 2 or 3 trials after reaching the admissible values of the relative errors in the boundary conditions (5) and (8). These errors, defined as

$$\delta_c = \left[\int_0^{2\pi} |v_r - v_0|^2 \, \mathrm{d}\varphi \Big/ \int_0^{2\pi} |v_0|^2 \, \mathrm{d}\varphi \right]^{1/2} \tag{14}$$

for the circle and

$$\delta_b = \left[\int_{-l/2}^{l/2} \left| v - \int G \Delta p \right|^2 \mathrm{d}x \Big/ \int_{-l/2}^{l/2} |v|^2 \, \mathrm{d}x \right]^{1/2} \tag{15}$$

for the beam, as well as the average relative error of the problem

$$\delta = \left[\int_0^{2\pi} |v_r - v_0|^2 \, a \, \mathrm{d}\varphi + \int_{-l/2}^{l/2} \left| v - \int G \Delta p \right|^2 \mathrm{d}x \right]^{1/2} \Big/ \times \left[\int_0^{2\pi} |v_0|^2 \, a \mathrm{d}\varphi + \int_{-l/2}^{l/2} |v|^2 \, \mathrm{d}x \right]^{1/2} \tag{16}$$

where computed on each run, so that it was possible to control the accuracy when necessary. If the errors (14) and (16) became larger than the admissible value, usually 0·2, the number of the equivalent sources was increased.

The following acoustic quantities were computed in the problem under study: complex power flow from the source contour C,

$$W = \frac{1}{2} \int_C p v_r^* a \, \mathrm{d}\varphi; \tag{17}$$

complex radiation impedance

$$Z = W / \langle v_0 \rangle^2, \tag{18}$$

where $\langle v_0 \rangle^2 = (1/2\pi) \int_0^{2\pi} |v_0|^2 \, \mathrm{d}\varphi$ is the mean squared value of the prescribed velocity; the power ratio PR defined as the active radiation power $\mathrm{Re}\, W$ normalized with the active radiation power $\mathrm{Re}\, W_0$ of the same source in free space [see also equation (4)]:

$$PR = 10 \log(\mathrm{Re}\, W / \mathrm{Re}\, W_0). \tag{19}$$

All the results presented below correspond to a circular sound source operating in water near a beam of steel. For definiteness, the beam thickness is equal to $h = 0{\cdot}2a$, and the material loss factor is $\eta = 0{\cdot}05$. For comparison, three particular cases of the problem were also considered. These are: a vibrating circle in free space (analytical solution for this case is well-known [11]), a circle near a perfectly rigid beam of length l [the Green function in equation (8) is equal to zero, $G = 0$], and a circle near the infinite rigid linear boundary.

Typical results of computation are presented in Figure 9. They correspond to a pulsating circle [$v_0 = \mathrm{const}$ in equation (5)], geometric parameters $l/a = 2$, H/a 1·5 and to the following numbers of the equivalent sources: $N_1 = 10$, $N_2 = 30$. Note that k is the acoustical wave number. It is seen from Figure 9(c) that the error in the boundary condition on the circular contour depends on frequency. It is maximum

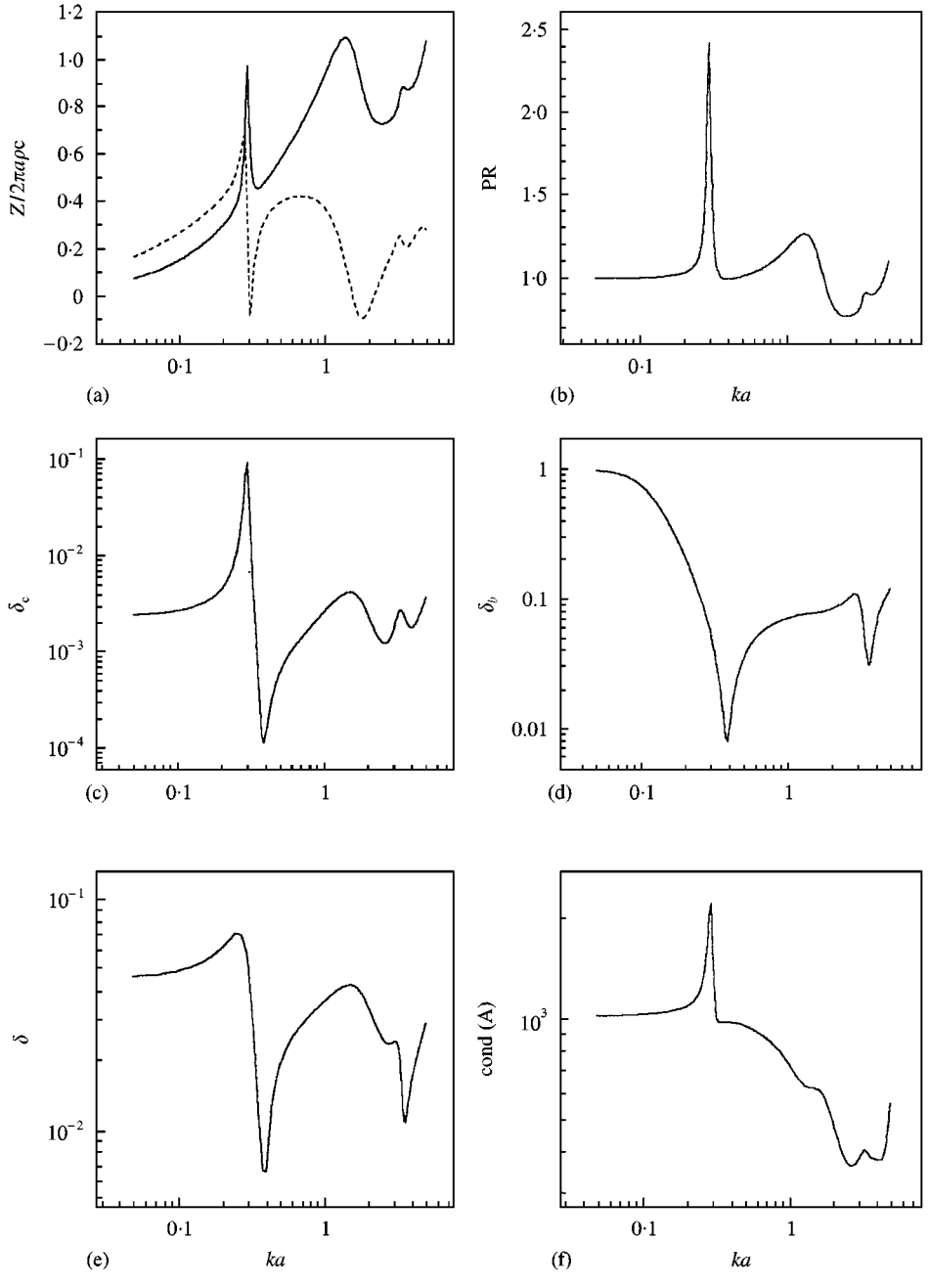

Figure 9. Specific radiation impedance (a), normalized power output *PR* (b), relative errors in the boundary conditions at the circle contour δ_c (c) and at the beam sides δ_b (d), average total error δ (e), and the condition number (f) for a circle pulsating in water near an elastic beam: $l = 2a$, $H = 1{\cdot}5a$, $m = 0$. Dotted line is for Imag Z.

at the resonance frequencies of the beam (10%); in the rest of the frequency region it does not exceed 10%. The error of equation (8) is also less than 10% everywhere except at very low frequencies [Figure 9(d)]. At these frequencies, the supported beam is very rigid and its velocity v is small. As a result, the relative error (15)

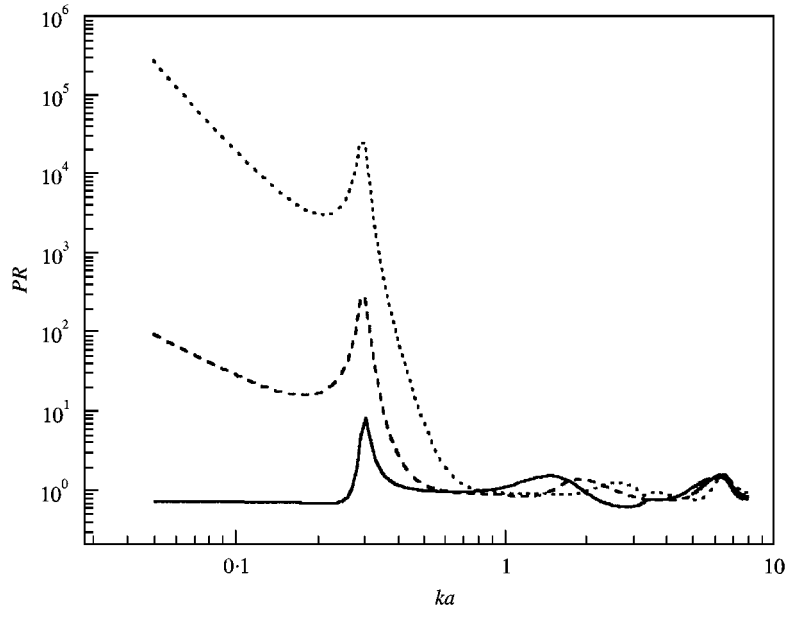

Figure 10. Power ratio (19) versus frequency of a circle near an elastic beam ($l = 2a$, $H = 1{\cdot}5a$) for the prescribed velocity $v_0(\varphi) = \sin\varphi$ (solid line), $\cos 2\varphi$ (dahsed line), and $\sin 3\varphi$ (dotted line).

becomes large though the absolute error is rather small and the average relative error (16) is quite acceptable. Figure 9(f) shows that the problem is rather ill-conditioned.

In what follows, the study is mostly confined to the power ratio PR as a function of frequency and to physical mechanisms of the power output amplification.

3.3. RESULTS

3.3.1. Resonant scattering

Beam resonance affects a good deal the sound power output of the circle. As is seen in Figure 9, the normalized power (19) which can also be interpreted as the coefficient of the source power amplification, has a distinct maximum at the frequency $ka = 0{\cdot}3$. This is the first eigenfrequency of the flexurally vibrating beam in water at which its length l is equal to a half-wavelength. For a pulsating cylinder, amplification at this frequency is 2·4. For sources of higher order m having the prescribed velocity (5) of the form $v_0 \sin(m\varphi)$ or $v_0 \cos(m\varphi)$, the amplification may be much greater. Figure 10 shows the power ratio (19) for $m = 1, 2, 3$ when the circle vibrates symmetrically with respect to the y-axis; see Figure 8. For the circle oscillating in the vertical direction ($m = 1$, solid line in Figure 10), the power amplification is about 10. For $m > 1$, the affect of resonant scattering is superimposed by another physical mechanism which is examined in detail in

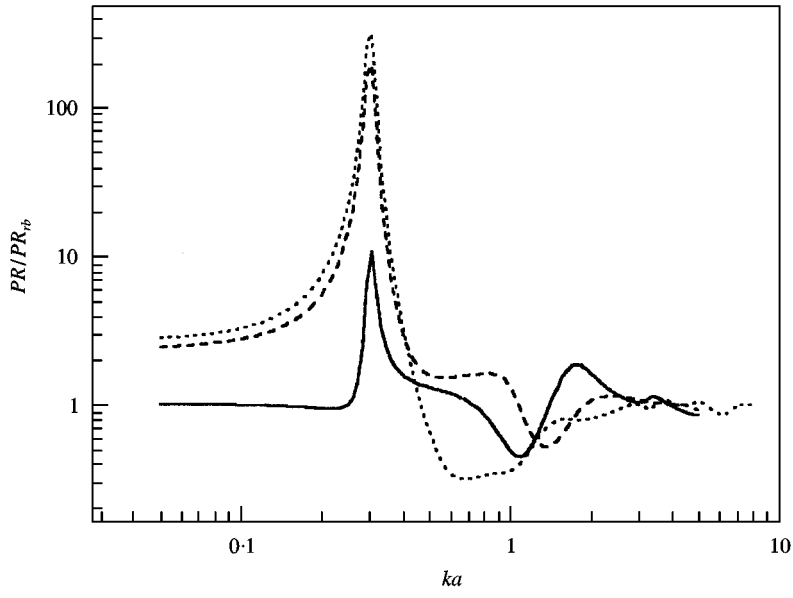

Figure 11. The power output of the circular source as in Figure 10 normalized with the power output Re W_{rb} of the same source near a rigid beam of similar geometry.

section 3.3.3. To purify the effect, the power curves in Figure 10 were normalized with the radiated power of the source operating near the perfectly rigid beam of the same geometry as that under study. The result is shown in Figure 11: the pure effect of the sound power amplification due to the first flexural resonance, $ka = 0{\cdot}3$, is 180 for $m = 2$ and 300 for $m = 3$. The increase of the power output with the source order m is explained as follows: less efficient sources have a stronger pressure near field which, acting on the elastic structure, excites higher levels of vibration and makes it reradiate more acoustic energy. It has been also verified that when the circular source vibrates antisymmetrically with respect to the y-axis, only the second eigenfrequency of the beam is excited at $ka = 1{\cdot}4$ (the beam length is equal to the wavelength), and the power amplification is equal to 1·05 for $m = 1$, 1·9 for $m = 2$, and 5·5 for $m = 3$: that is, much less than for symmetric case. Higher eigenfrequencies of the beam were not seen in the PR-curves. The authors did not manage to construct a velocity function $v_0(\varphi)$ in equation (5) which could noticeably excite the third or higher beam eigenfrequencies.

Thus, only the first eigenfrequency of the elastic beam, and partly the second one, are important for power output enhancement, the amplification coefficient being strongly dependent on the source order m and the minimal distance d between the source and beam, $d = H - a - h/2$. As is seen in Figure 11, for the source of order $m = 2$ and the distance $d = 0{\cdot}5a$, the coefficient of amplification is equal to 180. For large distances, $d > 5a$, the coefficient practically equals unity. But for smaller distances, $d < 0{\cdot}2a$, it exceeds 1000.

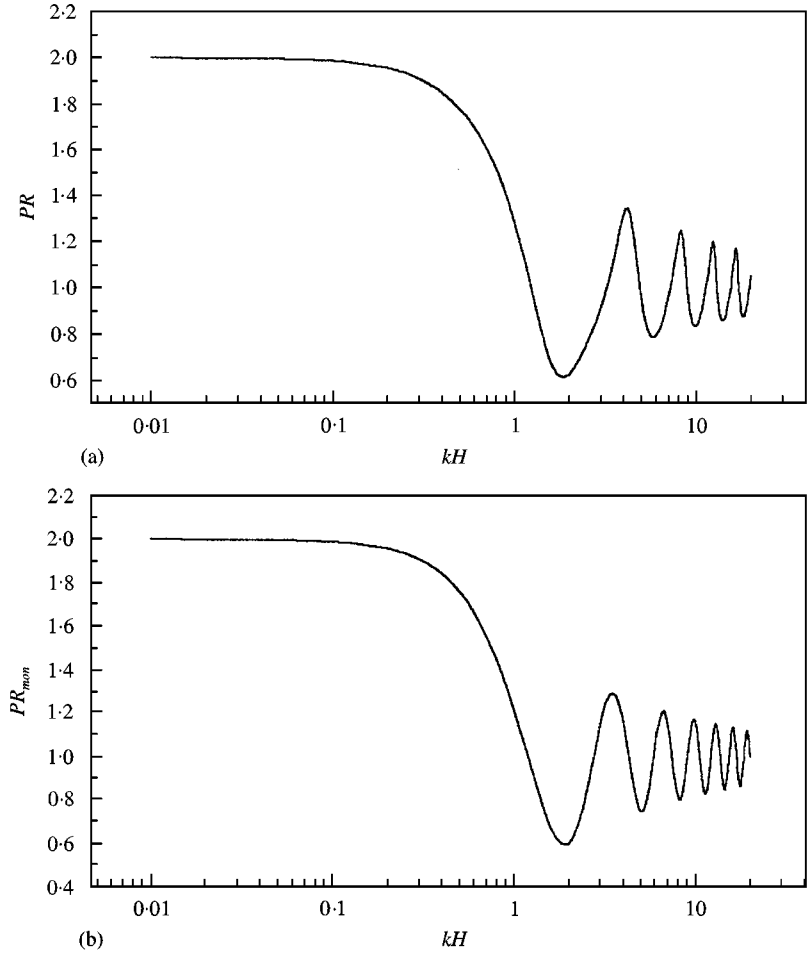

Figure 12. Power ratio (19) for a pulsating circle ($a = 0{\cdot}2H$) near a rigid infinite linear boundary (a) and for a point monopole source near the same boundary (b).

3.3.2. *Cavity resonance and interference*

Resonance of the cavity between the source and scatterer also affect the power output of the circular source. Here, this effect is not so large as, e.g., for a disc near a rigid plane [7], because of the curvature of the source surface. Besides, it is mixed with the interference effect. However, the effect exists and can be clearly observed for the elastic scatterer as well as for the rigid beam of finite length and infinite rigid line boundary.

As an example, Figure 12(a) shows the normalized radiation power as a function of frequency for a circle pulsating near an infinite rigid boundary. At low frequency, the power amplification is close to 2, and the main physical mechanism is interference of the direct and reflected waves: the pressure at the source surface in the reflected wave has the same amplitude and phase as that in the direct wave, so that the radiation resistance and power output are double the free-space values.

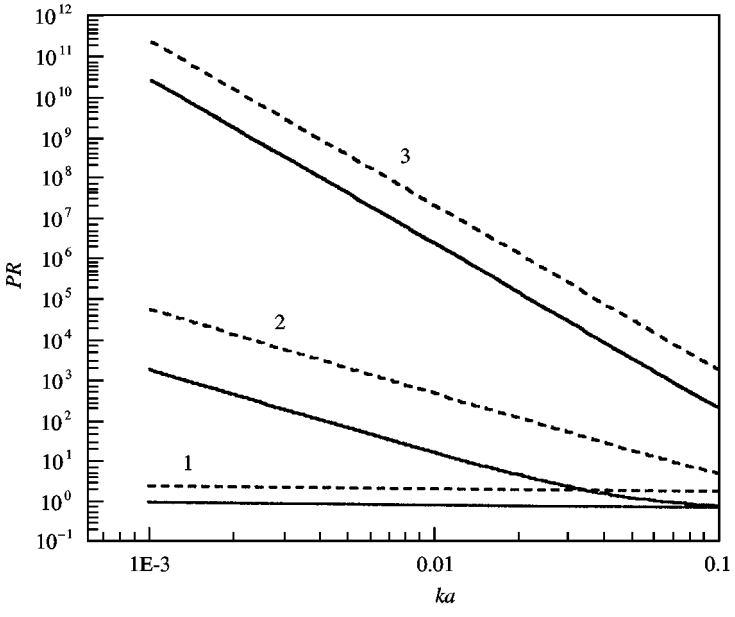

Figure 13. Power ratio (19) versus low frequency for a circle near an elastic beam with $l = 2a$, $H = 1.5a$ (solid lines) and near an infinite rigid linear boundary (dashed lines) for the prescribed velocity $v_0(\varphi) = \cos\varphi - 1$, $\sin 2\varphi - 2$, and $\cos 3\varphi - 3$.

At higher frequencies, the curve is determined mostly by cavity resonance: four small maxima of the curve correspond to the natural frequencies of the cavity, $kH \cong 4\pi n/3$, at which the minimal distance between the source and boundary, $d = 3H/4$, is approximately equal to the half-wavelength times the integer $n = 1$–4.

For comparison, in Figure 12(b), a similar curve is depicted for a point monopole source with the same volumetric velocity and at the same distance H from the rigid infinite boundary. At all frequencies, the only physical mechanism of the power output variation for a point source is the interference of the direct and reflected waves. Therefore, at low frequencies, the curve in Figure 12(b) is practically identical to the curve in Figure 12(a) but differs from it at higher frequencies being described by the formulae [13] $PR_{mon} = (1 + J_0(2kH))$, where J_0 is the Bessel function of zero order. Six maxima seen in Figure 12(b) correspond to the frequencies, $J_1(2kH) = 0$, at which the reflected wave comes back to the source in-phase with the volumetric velocity.

3.3.3. *Source order lowering*

A very interesting physical effect is observed in the low-frequency region–enormous amplification of the power output via the physical mechanism called here source order lowering. The effect takes place for poor radiators, i.e., for sources of high order m. It is clearly seen, e.g., in Figure 10 for the circular source with $m = 2$ and 3: the lower the frequency and the higher the source order, the greater the amplification coefficient. Figure 13 shows the effect at low frequencies for a circular

source (with $m = 1, 2, 3$) near a finite elastic beam (solid lines) and near an infinite rigid linear boundary (dashed lines). It is supposed that, for all m, the circle vibrates anti-symmetrically with respect to the y-axis. In free space, at very low frequencies these three sources are equivalent to the dipole, quadrupole and octupole point sources and their radiated power varies with frequency as ω^3, ω^5. and ω^7 respectively [11]. It follows from Figure 13 that the presence of the beam or rigid boundary makes all three sources radiate sound like a dipole source, in the sense that the radiated power of each of them becomes dependent on frequency as ω^3. In other words, a scatterer lowers the order m of a source down to unity.

A physical explanation of this effect is the following. Bringing the beam or other foreign body into a source vicinity breaks the rotational symmetry of the acoustic field. The antisymmetric vibration of the source urges the fluid between the source and scatterer to move to and fro in the horizontal direction. Such oscillating movement of fluid is equivalent to a dipole source, the radiation of which dominates in the total field.

It has been verified that when the circle vibrates near the beam symmetrically with respect to the y-axis, it radiates sound like a monopole source: the radiated power varies with frequency as ω^1. The power output amplification in this case is even higher than in Figure 13.

It is worth noting that the source order lowering mechanism is possible only for sources and scatterers of finite dimensions. With point sources this mechanism does not work.

4. MAIN RESULTS AND POSSIBLE APPLICATIONS

The aim of the work, which included an experimental as well as theoretical and numerical study, was to attract attention to the physical effect of increase in the power output of noise sources when they operate near boundaries or/and elastic structures.

In the *laboratory experiment* with a specially designed sound source and resonant scatterer, it was shown that the power increase is not an abstract "paper" effect but a matter of practice. As obtained in the experiment, the relative power increase due to the presence of the scattering object reached 100.

In the second part of the work, a *numerical solution* of the radiation problem for a noise source of finite dimensions near a finite elastic structure (the situation typical for industrial noise sources) was obtained. It was shown that the radiated power can reach orders of magnitude comparable with that of the same source operating in free space.

Four physical mechanisms of the power increase are formulated in this paper: interference of the direct and reflected waves; elastic structure resonance; resonance of the cavity between the source and scatterer; source order lowering.

The last mechanism, source order lowering, works at low frequencies with sound sources of high orders, i.e., the sources which are very inefficient radiators in free space, being equivalent to multipole point sources of high orders. A scatterer, whether rigid or elastic, lowers the source order and makes it radiate sound like

a monopole or dipole source. The effect of the power output amplification due to this mechanism is shown in the present paper to be extremely high—many orders of magnitude. Note that while the resonant scattering is frequency-selective the source order lowering is a broadband mechanism.

The results presented in this paper can be of practical importance in several ways. (1) In SEA, they may be helpful in finding appropriate corrections for the source power output. (2) In noise control, it is possible to design a reflection (scattering) environment near a sound source for reducing (or increasing) its radiation power. (3) The results might be useful for better understanding sound generation mechanisms in complicated industrial noise sources like, e.g., an automotive tyre which is an inefficient radiator in free space but rather noisy, perhaps due to the source order lowering, when operating near a reflecting plane (road) close to an elastic shell structure of the wheel house.

ACKNOWLEDGMENT

This research has been supported by the Swedish Research Council for Engineering Science (TFR) under grant #502323 and in part by the Russian Foundation for Basic Research under grant #980100552a. The authors are grateful to Prof. Tor Kihlman and Prof. Wolfgang Kropp for very valuable support and numerous discussions during the work and to Dr. Michael Korotkov for the essential contribution to the experiment.

REFERENCES

1. F. J. Fahy 1989 *Sound Intensity*. London: Elsevier Applied Science.
2. F. J. Fahy and W. G. Price (eds) 1997 *Proceedings of the IUTAM Symposium on SEA*. (*Southampton*, U.K. July.) Dordrecht: Kluwer Academic Publishers, 1999.
3. R. V. Waterhouse 1958 *Journal of the Acoustical Society of America* **30**, 4–13. Output of a sound source in a reverberation chamber and other reflecting environments.
4. P. M. Morse and K. U. Ingard 1968 *Theoretical Acoustics*. New York: McGraw-Hill Book Company.
5. G. H. Schmidt 1977 *Journal of Sound and Vibration* **53**, 289–300. Influence of an unbounded elastic plate on the radiation of sound by a point source.
6. S. N. Yousri and F. J. Fahy 1974 *Journal of Sound and Vibration* **32**, 311–325. An analysis of acoustic power radiated into a reverberation chamber by a transversely vibrating slender bar.
7. T. M Tomilina 1996 *Proceedings INTER-NOISE 96 Conference*, *Liverpool*, *U.K.*, *August*) **6**, 3149–3153. Amplification of the total power flow from a noise source operating near elastic bounds.
8. K. F. Graff 1975 *Wave Motion in Elastic Solids*. Oxford: Clarendon Press.
9. Yu. I. Bobrovnitskii and T. M. Tomilina 1990 *Soviet Physics – Acoustics*, **36**, 334–338. Calculation of radiation from finite elastic bodies by the method of auxiliary sources.
10. T. M. Tomilina 1989 *Proceedings of the 13th International Congress on Acoustics*, *Belgrade*, *Yugoslavia*, **4**, 443–446. Fast algorithm for sound field analysis based on the Equivalent Sources Method.
11. E. Skudrzyk 1971 *The Foundations of Acoustics*. Wien: Springer-Verlag.
12. H. Hönl, A. W. Maue and K. Westpfahl 1961 *Theorie der Beugung*. Berlin: Springer.
13. M. C. Junger and D. Feit 1993 *Sound. Structures, and their Interaction* New York: Acoustical Society of America.